Inter-annual and decadal variability on the sea level around the China seas

Ying Qu (quying.bnu.cn@gmail.com)
Suzhou University of Science and Technology
Chao Yue
Beijing Normal University
Anboyu Guo
National Marine Environmental Forecasting Center

Research Article

Keywords: sea level, Inter-annual and decadal variability, ENSO, PDO

Posted Date: May 20th, 2022

DOI: https://doi.org/10.21203/rs.3.rs-1640679/v1

Abstract

All tide gauge stations around the China seas can be divided into two subregions according to their correlations before and after removing the seasonal cycle, within which the stations generally have very high correlations with each other. Region 1 is located in the Bohai Sea, the Yellow Sea, the East China Sea, and adjacent areas of China, which are in Korea and Japan; Region 2 is located in the South China Sea. EOF decomposition is performed on the tide gauge records within each subregion after removing the vertical land motion and the seasonal cycle, and then do the wavelet coherence analysis between the principal component (PC) time series of each subregion and the Southern Oscillation Index (SOI) as well as the Pacific Decadal Oscillation (PDO) time series. Results show that the first PC time series of Region 1 has no significant coherence with the SOI index on inter-annual timescales, but it proves strong coherence in the 8-to-16-year band; in contrast, the inter-annual variation of the sea level in the Region 2, which is mainly represented by the first mode, is consistent with the change of SOI revealing that the inter-annual variation of sea level in the South China Sea is closely related to ENSO. The wavelet coherence between the first PC time series of Region 1 and PDO index shows that they have strong coherence in the 8-to-16-year band. The wavelet coherence between the first PC time series of Region 2 and PDO index shows strong coherence in the 8-to-16-year band, and during 2000–2016, they also have strong coherence in the 3-to-7-year band.

1. Introduction

Inter-annual and decadal climate fluctuations such as El Niño-Southern Oscillation (ENSO) and Pacific Decadal Oscillation (PDO) may impact the variations of sea level on regional scales with considerably higher amplitudes (Calafat et al., 2013). China has a coastline spread over 32 kilometers, high density of population and infrastructures place it in a vulnerable position under the circumstances of climate change (Han et al., 1997; Chen, 1997; Shi et al., 2000; Wang et al., 2012), thus, it is of vital significance to analyze the mechanism of ENSO and PDO working on the sea level around the China seas.

For the China coast, the South China Sea is the largest marginal sea in Southeast Asia which is a semi-closed basin surrounded by southern China, the Philippines, Borneo island, and China-Indochina Peninsula. Due to the special geographical location of the South China Sea, there have been a large number of studies on the mechanism of sea level variability in the South China Sea on inter-annual and longer time scales (Qu et al., 2000; Qu et al., 2004; Rong et al., 2007), indicating that the inter-annual change of sea level in the South China Sea is closely related to ENSO and decadal PDO (Mohan and vethamony, 2017). ENSO can also affect the sea level variations of the Yellow Sea, the Bohai Sea, and the East China Sea through the action of wind stress (Han et al., 2020; Li et al., 2016; Zuo et al., 2012). Liu et al. (2009) used satellite altimetry data from 1992 to 2007 to analyze the relationship between sea level anomalies in the Yangtze River Estuary as well as the Southern East China Sea and ENSO respectively, calculated the correlation coefficient between the low-frequency component of sea level anomalies and the southern oscillation index, and found that the sea level anomalies in the two regions are regulated by ENSO, further analysis show that ENSO affects the wind stress field through the atmospheric circulation,

and then influences the sea level variations. Decadal sea level variations in the Yellow Sea, the Bohai Sea, and the East China Sea are associated with PDO by a significant inverse correlation between them (Han and Huang, 2008).

Many studies have been done on the analysis of sea level variability for some parts of the China seas, especially in the South China Sea. However, due to the lack of tide gauge records and the short temporal coverage of satellite altimetry, the inter-annual and decadal variations of sea level for the whole China seas on different time and spatial scales still needs to be further explored.

In this paper, 25 tide gauge records are used to study the inter-annual and decadal sea level variability around the China seas, the wavelet coherence method is used along with ENSO and PDO index to study the response of sea level variations to the dynamic processes of the ocean (Han and Huang, 2008).

2. Data And Methods

2.1 Data

Monthly tide gauge data are obtained from the Permanent Service for Mean Sea level (PSMSL) (Holgate et al., 2013; PSMSL, 2017). 25 tide gauge records covering different periods along the Chinese coast are selected, detailed information is shown in Table 1.

Table 1
Tide gauge records along the Chinese coast

Station number	Station Name	Time span
1	Dalian	1970–2016
2	Qinhuangdao	1950–1994
3	Yantai	1954–1994
4	Lusi	1967–2016
5	Keelung □	1956–1995
6	Incheon	1960–2016
7	Mokpo	1960–2016
8	Jeju	1964–2016
9	Sasebo □	1966–2016
10	Nagasaki	1965–2016
11	Fukue	1965–2016
12	Kuchinotsu	1975–2016
13	Akune	1970–2016
14	Odomari	1965–2016
15	Nisinoomote	1965–2016
16	Naha	1966–2016
17	Kanmen	1959–2016
18	Xiamen	1954–2004
19	Macau	1925–1985
20	Tsim bei tsui	1974–2016
21	Tai po kau	1963–2016
22	NPQB	1950–2016
23	Chi ma wan	1961–1997
24	Zhapo	1959–2016
25	Hondau	1957–2013

We calculate the correlation coefficients between all 25 tide gauges before and after removing the seasonal cycle (Fig. 1). When the seasonal cycle is included, the stations can be divided into two

subregions within which the stations generally have very high correlations with each other: Region 1, the Bohai Sea, the Yellow Sea, the East China Sea, and adjacent waters, which comprises stations 1–17 (identified in Table 1); Region 2, the South China Sea, contains stations 18–25. After removing the seasonal cycle from all stations, the correlations both within, and between the two regions, are all reduced to some extent. Regions are much more differentiated from each other after the seasonal cycle is removed except for stations 9–13. Thus, seasonal cycles account for more of the intra-regional correlations in both regions.

Region 1 covers the Bohai Sea, the Yellow Sea, and the East China Sea while Region 2 is in the South China Sea where the seasonal character is quite different from Region 1. Figure 2 shows all tide gauge stations in both regions.

Figure 2 shows the seasonal amplitude of tide gauge record at each location in Region 1 and Region 2. The seasonal amplitudes of most tide gauges in Region 1 are larger than Region 2. Among all stations, Qinhuangdao has the largest amplitude. Figure 3 presents the tide gauge record after removing the seasonal cycle at each location.

The SOI is a kind of commonly used ENSO index calculated from the sea level pressure difference between Tahiti and Darwin, located in Australia. It is a means to observe the large-scale fluctuations in air pressure between the western and eastern of the equatorial Pacific and to characterize the development state and intensity of El Niño and La Niña events. The SOI time series correspond well with ocean temperature changes across the eastern tropical Pacific. The positive (negative) SOI phase coincides with abnormally cold (warm) ocean waters across the equatorial eastern Pacific and the enhancement of the Pacific trade wind, which are typical of La Niña (El Niño) events.

The PDO is regarded as a long-lived El Niño-like pattern of Pacific climate variation. It is defined as the leading principal mode of monthly sea surface temperature variations of North Pacific (poleward of 20°N). The positive phase of PDO is associated with cool waters in the midlatitude North Pacific and intensified Aleutian low along with strong westerlies (Gordon and Giulivi, 2004; Mantua et al., 1997).

The monthly time series of ENSO and PDO index are obtained from NOAA. (https://www.ncei.noaa.gov/access/monitoring/products/).

2.2 Methods

In this analysis, the wavelet coherence method is applied to determine the correlation coefficient in time frequency space following Grinsted et al (2004):

$$R_n^2(s) = \frac{\left|S\left(s^{-1}W_n^{xy}(\mathrm{s})\right)\right|^2}{S\left(s^{-1}\left|W_n^x(s)\right|^2\right)\cdot S\left(s^{-1}\left|W_n^y(s)\right|^2\right)}$$

1

S is a smoothing operator while $W_n^X(s)$ can be regarded as the local phase.

To remove the trend of vertical land motion (VLM) from tide gauge records, we calculate the difference between monthly sea level anomalies measured by satellite altimetry and tide gauge records at each location for 1993–2018. Sea level anomalies are obtained from AVISO (Archiving, Validation, and Interpretation of Satellite Oceanographic Data) on a resolution of 0.25°×0.25°. As no GPS data are available in mainland China, so here we use the substitute method because satellite altimetry is not influenced by VLM, while tide gauge records include VLM. (Kuo et al., 2004; Ostanciaux et al., 2012; Chen et al., 2018).

3. Results

3.1 Sea level variability responses to ENSO

Sea surface temperatures along the coast in our study area have a close relationship with ENSO, which will then influence the sea level variability. We perform EOF analysis on all the 14 tide gauge stations corrected for VLM in Region 1. After removing VLM, the linear trend and the seasonal cycle from the SLC time series, the first three leading principal components and their eigenvectors are shown in Fig. 4. The first EOF mode accounts for 52.6% of the variance, while the second accounts for 10.0%, and the third EOF accounts for 9.0% of the total variance.

Figure 5 presents the wavelet coherence between SOI and the amplitude time series of the first EOF of Region 1, PC1. Figure 5a shows that the two series vary coherently, generally, positive SOI (i.e., La Niña events) correlating with positive amplitudes of PC1 time series while negative SOI (i.e., El Niño events) correlating with negative amplitudes of PC1 time series in Region 1. Figure 5b presents the wavelet coherence between SOI and PC1, and the results show that SOI and PC1 time series have significant ($p < 0.05$, against red noise) coherence in the 8-to-16-year band during 1980–2016, and the PC1 time series leads the SOI by 1/4 of the period. Therefore, it can be inferred that the impact of ENSO on sea level variations in the East China Sea, the Yellow Sea, the Bohai Sea, and adjacent waters are mainly on decadal or longer time scales.

We also perform EOF analysis on all tide gauge records in Region 2 after removing the linear trend, the VLM, and the seasonal cycle, the results are shown in Fig. 6. The variance explained by the first three principal modes are 66.5%, 20.7% and 8.5%, respectively. Figure 7 shows the wavelet coherence between the amplitude time series of the first principal mode (PC1) of Region 2 and SOI. Figure 7a also shows that the two series vary coherently, positive SOI correlating with positive amplitudes of PC1 time series and negative SOI correlating with negative amplitudes of PC1 time series, but also there are some opposite examples such as negative SOI correlating with high amplitudes (e.g., 1997). Figure 7b shows that wavelet coherence between PC1 time series and SOI has significant, in-phase relationship in the 3-to-7-

year band during 1995–2015, also it is significant and in-phase in the 10-to-16-year band during 1980–2016. Thus, there is a strong coherence between SOI and PC1 on timescales from inter-annual to decadal.

As the South China Sea is a semi-closed ocean basin that exchanges water with adjacent waters, including the East China Sea, the Sulu Sea, the Java Sea and the Pacific Ocean, the adjacent seas and the Pacific Ocean must play an essential role in its sea level variability, on not only seasonal timescale, but also on inter-annual timescale and longer timescales. At the developing stage of El Niño, there is increased Luzon Strait transport flowing into the South China Sea, while higher temperature water flows out of the South China Sea through the Mindoro Strait and the Balabec Strait (Qu et al., 2000; Qu et al., 2004; Rong et al., 2007) which cools the South China Sea and even results in lower sea level, but at the developing stage of La Niña, the situation is reversed. The southwesterly monsoon also plays a role via its impact on ocean circulation. In summer, when at the developing stage of El Niño, the Western Pacific subtropical high leads to cyclonic wind anomalies, which drive water divergence in the South China Sea, cooling it and then thinning the mixed layer, thus less heat is stored lowering sea level, Still, at the developing stage of La Niña, the situation is reversed, warm water convergence deepens the mixed layer, raising sea level (Huang et al., 2004; Rong et al., 2007).

3.2 Sea level variability responses to PDO

The above studies revealed that sea level variations in Region 1 and Region 2 are affected by the changes in the Pacific Ocean on decadal scale, that is, PDO. PDO can also be regarded as a response to ENSO and atmospheric noise (Schneider and Cornuelle, 2005; Newman et al., 2003), and they are closely correlated in the low frequency band (Zhang and church, 2012). PDO can affect the intensity and frequency of ENSO. In this analysis, wavelet coherence method is adopted to analyze the correlation between PDO and ENSO. The results are shown in Fig. 8, in which Fig. 8a is the comparison between the time series of SOI and PDO, and Fig. 8b is the wavelet coherence of the two time series. It can be found in Fig. 8a that there is an obvious anti-correlation between the time series of SOI and PDO, positive SOI generally correlating with negative PDO. Figure 8b shows that the SOI time series and PDO time series have strong coherence on multiple time scales. The two time series are highly correlated from 1980 to 1990 in the two-year band with SOI leading PDO, which means, SOI may drive PDO. Also, the two series have strong anti-phase coherence in the band of 4-to-16-year from 1980 to 2016. Overall, PDO is closely related to or affected by SOI on multiple time scales.

The wavelet coherence between the PC1 time series of Region 1 and PDO is shown in Fig. 9a, and that between the PC1 time series of Region 2 and PDO is shown in Fig. 9.b. It can be seen in Fig. 9a that, the wavelet coherence between PC1 time series of Region 1 and PDO has strong anti-phase coherence in the 8-to-16-year band from 1980 to 2016. When PDO is positive, relatively low sea level is found in the East China Sea, the Yellow Sea, the Bohai Sea, and adjacent areas including Japan and Korea. When PDO is negative, high sea level is found there. During a positive PDO phase, the Aleutian low pressure becomes deeper and moves southward, while the westerlies in the North Pacific strengthen, resulting in the increasement of Ekman transport to the South, which leads to the reduction of sea surface temperature in the mid-latitude Pacific, so the steric sea level and sea surface height are relatively low and vice versa.

The influence of PDO on the sea level variations in the Northwest Pacific is also considered to be related with the Kuroshio geostrophic transport (Gordon and Giulivi, 2004). The Kuroshio geostrophic transport affects the sea level difference between the Japan/East Sea and the subtropical North Pacific. Comparison between the Kuroshio and PDO reveal that when the transport is large, the sea level slope across both sides of the Kuroshio is large, which corresponds to the positive phase of PDO; When the transport is small, the sea level slope across both sides of the Kuroshio is also relatively small, which corresponds to the negative phase of PDO. In addition, PDO influencing the sea level variations in the East China Sea and Yellow Sea is also considered to be related to the runoff of the Yangtze River (Han and Huang, 2008). Since the Yangtze River is the main source of freshwater runoff to the East China Sea and Yellow Sea, the changes of runoff can significantly affect the distribution of seawater salinity in this region, and then affect the steric sea level variations.

The wavelet coherence between the PC1 time series of Region 2 and PDO shows strong anti-phase coherence in the 8-to-16-year band from 1980 to 2016, as well as strong anti-phase coherence in the 3-to-7-year band during the period of 2000–2016. When PDO is in the positive phase, sea level in the South China Sea is relatively low, and the negative phase of PDO corresponds to the high sea level. This may be due to the strengthening of easterly trade related to PDO (Merrifield et al., 2012; Cheng et al., 2016). In PDO negative-phase years, the intensified easterly trade wind and negative wind stress curl deepen the thermocline thickness of the western tropical Pacific, so the steric sea level and total sea level are at a high level, and vice versa.

4. Results And Discussion

In this study, to analyze the inter-annual and decadal variations of sea level around the China seas, 25 tide gauge records in the study area are used, we calculate the correlation coefficients between all tide gauge records before and after removing the seasonal cycle. It is found that the all stations can be divided into two subregions, one is Region 1, which is located in the Bohai Sea, the Yellow Sea, the East China Sea and the adjacent regions, including South Korea and Japan; another is Region 2, that is the South China Sea.

EOF analysis is performed on 14 tide gauge records after correcting the VLM and the seasonal cycle in Region 1. The first mode accounts for 52.6% of the variance, while the second accounts for 10.0% and the third EOF accounts for 9.0% of the total variance. We also perform EOF analysis on the tide gauge records after removing the VLM and the seasonal cycle in Region 2, the explained variance of the first three principal modes are 66.5%, 20.7% and 8.5%, respectively. Then wavelet coherence method is utilized to analyze the inter-annual and decadal variability on sea level in Region 1 and Region 2 respectively.

The wavelet coherence analysis between the amplitude time series of PC1 in Region 1 and the SOI index time series shows that they have no significant coherence on interannual timescales but it proves strong coherence in the 8-to-16-year band. Thus, the influence of ENSO on the sea level variability in Region 1 is mainly on the ultra-low frequency. The wavelet coherence analysis is also performed between the

amplitude time series of PC1 in Region 2 and the SOI index time series, it is found that from 1995 to 2015, they have strong coherence in the band of 3-to-7-year, and from 1980 to 2016, they also have a significant in-phase relationship in the band of 10-to-16-year. That is, the inter-annual and decadal changes of sea level in the South China Sea are closely related to ENSO.

The decadal variations of sea level around the China seas are studied by wavelet coherence analysis between the PC1 times series of Region 1 as well as Region 2 and the PDO index time series respectively. The results show that decadal sea level variability in Region 1 and PDO have strong coherence in the 8-to-16-year band from 1980 to 2016, so does Region 2, Region 2 and PDO also have strong coherence in the 3-to-7-year band from 2000 to 2016.

The inter-annual and decadal variability of sea level around the China seas are related to PDO and ENSO, while PDO and ENSO also have an internal relationship (Pei et al., 2015), which means an internal relation between the tropical Pacific and the North Pacific in affecting the sea level variation around the China seas, and the mechanism of the interaction remains to be further discussed.

Declarations

Data availability

The tide gauge records can be found at: https://doi.org/10.5281/zenodo.6534154. The wavelet coherence method can be found at: https://doi.org/10.5281/zenodo.6534145

Ethics declarations

Competing interests

The authors declare that they have no competing interests.

Acknowledgements:

We are grateful for data from Permanent Service for Mean Sea Level (PSMSL), 2020, "Tide Gauge Data", Retrieved 19 Oct 2020 from http://www.psmsl.org/data/obtaining/.

Funding:

Ying Qu thanks for funding from State Key Laboratory of Cryospheric Science, Northwest Institute of Eco-Environment and Resources, Chinese Academy Sciences (Grant Number: SKLCS-OP-2020-07).

Authors' contributions:

Ying Qu processed the data and wrote the paper, Yuechao and Anboyu Guo provided insights into the methods. All authors have read and approved the final manuscript.

Author information:

Ying Qu[1,2,3], Chao Yue[3], Anboyu Guo[4]

1. School of Geography Science and Geomatics Engineering, Suzhou University of Science and Technology, Suzhou, 215009, China

2. State Key Laboratory of Cryospheric Science, Northwest Institute of Eco-Environment and Resources, Chinese Academy of Sciences, Lanzhou 730000, China

3. College of Global Change and Earth System Science, Beijing Normal University, Beijing, China

4. National Marine Environmental Forecasting Center, Beijing, China

Corresponding author:

Correspondence to Ying Qu.

Publisher's Note

References

1. Holgate SJ, Matthews A, Woodworth PL, Rickards LJ, Tamisiea ME, Bradshaw E, Foden PR, Gordon KM, Jevrejeva S, Pugh J (2013) New data systems and products at the permanent service for mean sea level. J Coastal Res 29(3):493–504. https://doi:10.2112/JCOASTRES-D-12-00175.1
2. Calafat FM, Chambers DP, Tsimplis MN (2013) Inter-annual to decadal sea-level variability in the coastal zones of the Norwegian and Siberian Seas: The role of atmospheric forcing. J Geophys Res: Oceans 118:1287–1301. doi:10.1002/jgrc.20106
3. Chen J (1997) The Impact of Sea level Rise on China's Coastal Areas and Its Disaster Hazard Evaluation. J. Coastal Res. 2050, 925–930
4. Chen N, Han G, Yang J (2018) Mean relative sea level rise along the coasts of the China Seas from mid-20th to 21st centuries. Cont Shelf Res 152:27–34. https://doi.org/10.1016/j.csr.2017.12.002
5. Cheng X, Xie S-P, Du Y, Wang J, Chen X, Wang J (2016a) Interannual-to-decadal variability and trends of sea level in the South China Sea. Clim Dyn 46:3113–3126
6. Church JA, Woodworth P, Aarup T, Wilson WS (2010) Understanding sea-level rise and variability. Wiley, London
7. Cummins PF, Lagerloef GSE, Mitchum G (2005) A regional index of northeast Pacific variability based on satellite altimeter data. Geophys Res Lett 32:L17607
8. Fang G, Chen H, Wei Z et al (2006) Trends and interannual variability of the South China Sea surface winds, surface height, and surface temperature in the recent decades. J Geophys Res 111:C11S16. https://doi.org/10.1029/2005JC003276

9. Gordon AL, Giulivi CF (2004) Pacific decadal oscillation and sea level in the Japan/East Sea. Deep-Sea Res I 51:653–663
10. Grinsted A, Moore JC, Jevrejeva S (2004) Application of the cross wavelet transform and wavelet coherence to geophysical time series. Nonlinear Process Geophys 11:561–566
11. Hamlington BD, Quan XW, Leben RR (2013) Intensification of decadal and multi-decadal sea level variability in the western tropical Pacific during recent decades. Clim Dyn 43:1357–1379. https://doi.org/10.1007/s00382-013-1951-1
12. Han M, Hou J, Wu L (1997) Potential Impacts of Sea level Rise on China's Coastal Environment and Cities: A National Assessment.J. Coastal Res. (14),79–95
13. Han G, Huang W (2008) Pacific decadal oscillation and sea level variability in the Bohai, Yellow, and East China seas. J Phys Oceanogr 38(12):2772–2783
14. Han G, Huang W (2009) Low-frequency sea-level variability in the South China Sea and its relationship to ENSO. Theor Appl Climatol 97:41–52
15. Han M, Nam S, Cho Y-K, Kang H-W, Jeong K-Y, Lee E (2020) Interannual Variability of Winter Sea Levels Induced by Local Wind Stress in the Northeast Asian Marginal Seas: 1993–2017. J Mar Sci Eng 8:774. https://doi.org/10.3390/jmse8100774
16. Kuo CY, Shum CK, Braun A, Mitrovica JX (2003) Vertical crustal motion determined by satellite altimetry and tide gauge data in Fennoscandia. Geophys Res Lett 31(1):1–4. https://doi.org/10.1029/2003GL019106
17. Li Y, Zuo J, Lu Q, Zhang H, Chen M (2016) Impacts of wind forcing on sea level variations in the East China Sea: local and remote effects. J Mar Syst 154:172–180. https://doi.org/10.1016/j.jmarsys.2015.10.009
18. Liu X, Liu Y, Guo L, Rong Z, Gu Y, Liu Y (2010) Interannual changes of sea level in the two regions of East China Sea and different responses to ENSO. Global Planet Change 72:215–226. https://doi.org/10.1016/j.gloplacha.2010.04.009
19. Mantua NJ, Hare SR, Zhang Y, Wallace JM, Francis RC (1997) A Pacific interdecadal climate oscillation with impacts on salmon production. Bull Am Meteorol Soc 78:1069–1079
20. Marcos M, Tsimplis MN, Calafat FM (2012) Inter-annual and decadal sea level variations in the north-western Pacific marginal seas. Prog Oceanogr 105:4–21
21. Merrifield MA, Thompson PR, Lander M (2012) Multidecadal sea level anomalies and trends in the western tropical Pacific. Geophys Res Lett 39:L13602. doi:10.1029/2012GL052032
22. Moon JH, Song YT (2017) Decadal sea level variability in the East China Sea linked to the North Pacific Gyre Oscillation. Cont Shelf Res 143:278–285. https://doi.org/10.1016/j.csr.2016.05.003
23. Newman M, Compo GP, Alexander MA (2003) ENSO-forced variability of the Pacific decadal oscillation. J Clim 16(23):3853–3857
24. Ostanciaux É, Husson L, Choblet G, Robin C, Pedoja K (2012) Present-day trends of vertical ground motion along the coast lines. Earth-Sci Rev 110(1–4):74–92.

https://doi.org/10.1016/j.earscirev.2011.10.004

25. Pei YH, Zhang RH, Zhang. XM, Jiang LH, Wei YZ (2015) Variability of sea surface height in the South China Sea and its relationship to Pacific oscillations. 34:80–92. https://doi.org/10.1007/s13131-015-0773-x. 12
26. Rong Z, Liu Y, Zong H, Cheng Y (2007) Interannual sea level variability in the South China Sea and its response to ENSO. Glob Planet Change 55(4):257–272. https:// doi.org/10.1016/j.gloplacha. 2006.08.001
27. Schneider N, Cornuelle BD (2005) The forcing of the Pacific Decadal Oscillation. J Clim 18:4355–4373. doi:10.1175/JCLI3527.1
28. Shi YF, Zhu JW, Xie ZR, Ji ZX, Jiang ZX, Yang GS (2000) Prediction and prevention of the impacts of sea level rise on the Yangtze River Delta and its adjacent areas. Sci China (Series D) 43(4):412–422
29. Soumya M, Vethamony P, Tkalich P (2015) Inter-annual sea level variability in the southern South China Sea. Global Planet Change 133:17–26
30. Wang J, Gao W, Xu SY, Yu LZ (2012) Evaluation of the combined risk of sea level rise, land subsidence, and storm surges on the coastal areas of Shanghai. China Clim Change 115(3–4):537–558. https://doi.org/10.1007/s10584-012-0468-7
31. Wang H, Liu KX, Wang AM, Feng JL, Fan WJ, Liu QL, Xu Y, Zhang ZJ (2018) Regional characteristics of the effects of the El Nino-Southern Oscillation on the sea level in the China Sea. Ocean Dyn 68(4–5):485–495
32. Wu Q, Zhang X, Church JA, Hu J (2017) Variability and change of sea level and its components in the Indo-Pacific region during the altimetry era. J Geophys Res Oceans 122:1862–1881. https://doi.org/10.1002/2016JC012345
33. Zhang X, Church JA (2012) Sea level trends, interannual and decadal variability in the Pacific Ocean. Geophys Res Lett 39(21):653–660
34. Zuo J, He Q, Chen C, Chen M, Xu Q (2012) Sea level variability in the East China Sea and its response to ENSO. Water Sci Eng 5(2):1–6
35. Zhang, X., Church, J.A., 2012. Sea level trends, interannual and decadal variability in the Pacific Ocean. Geophysical Research Letters, 39(21): 653–660.
36. Zuo, J., He, Q., Chen, C., Chen, M., Xu, Q., 2012. Sea level variability in the East China Sea and its response to ENSO. Water Sci. Eng. 5 (2), 1–6.

Figures

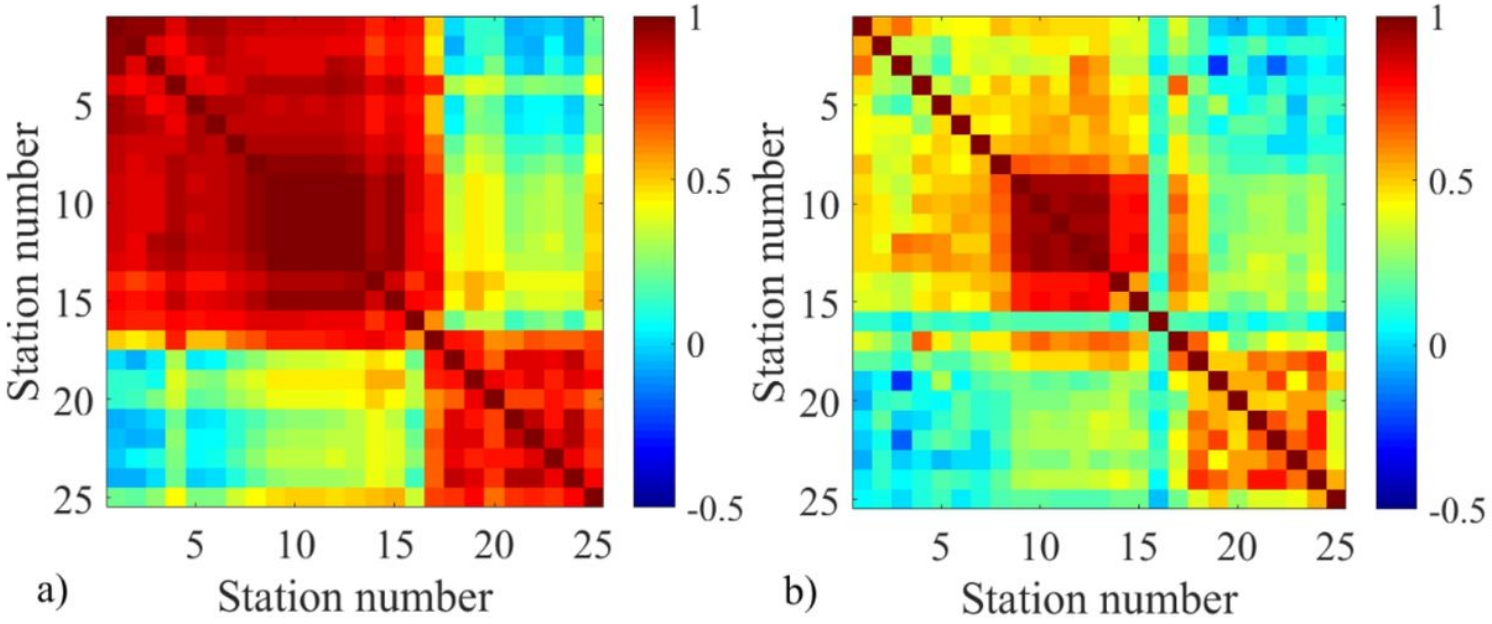

Figure 1

a) The correlation between the 25 tide gauge stations b) correlations after removing the seasonal cycle

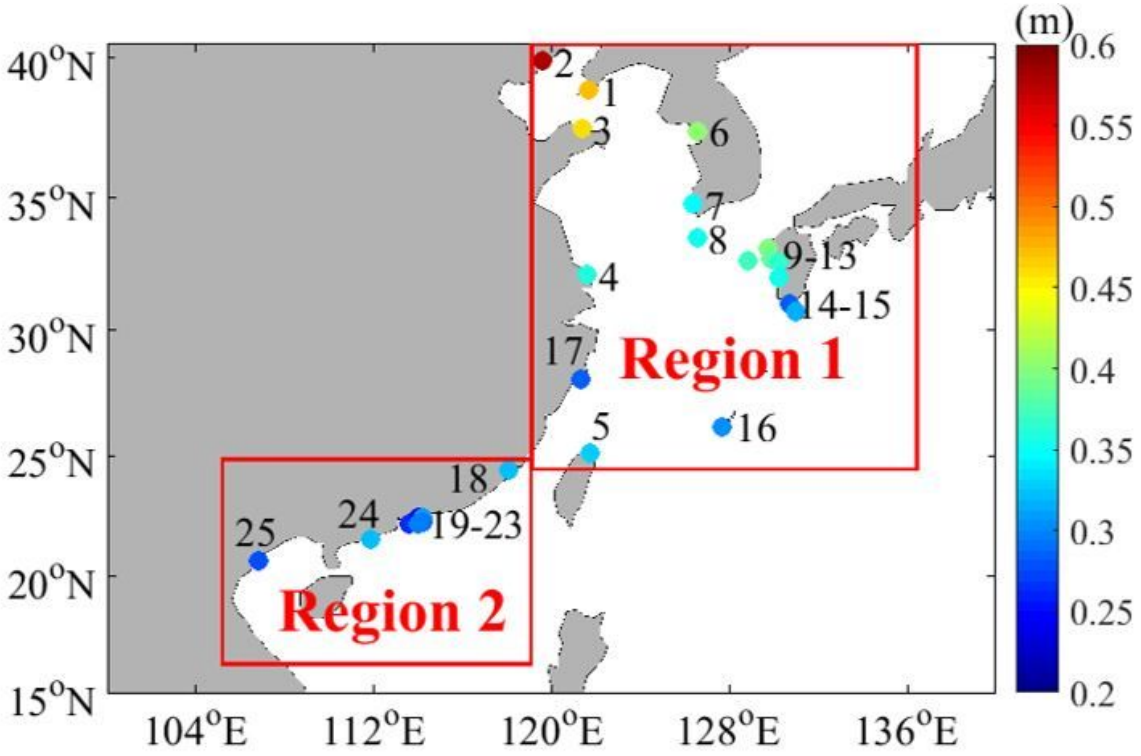

Figure 2

The seasonal amplitude at each tide gauge station (Units: m)

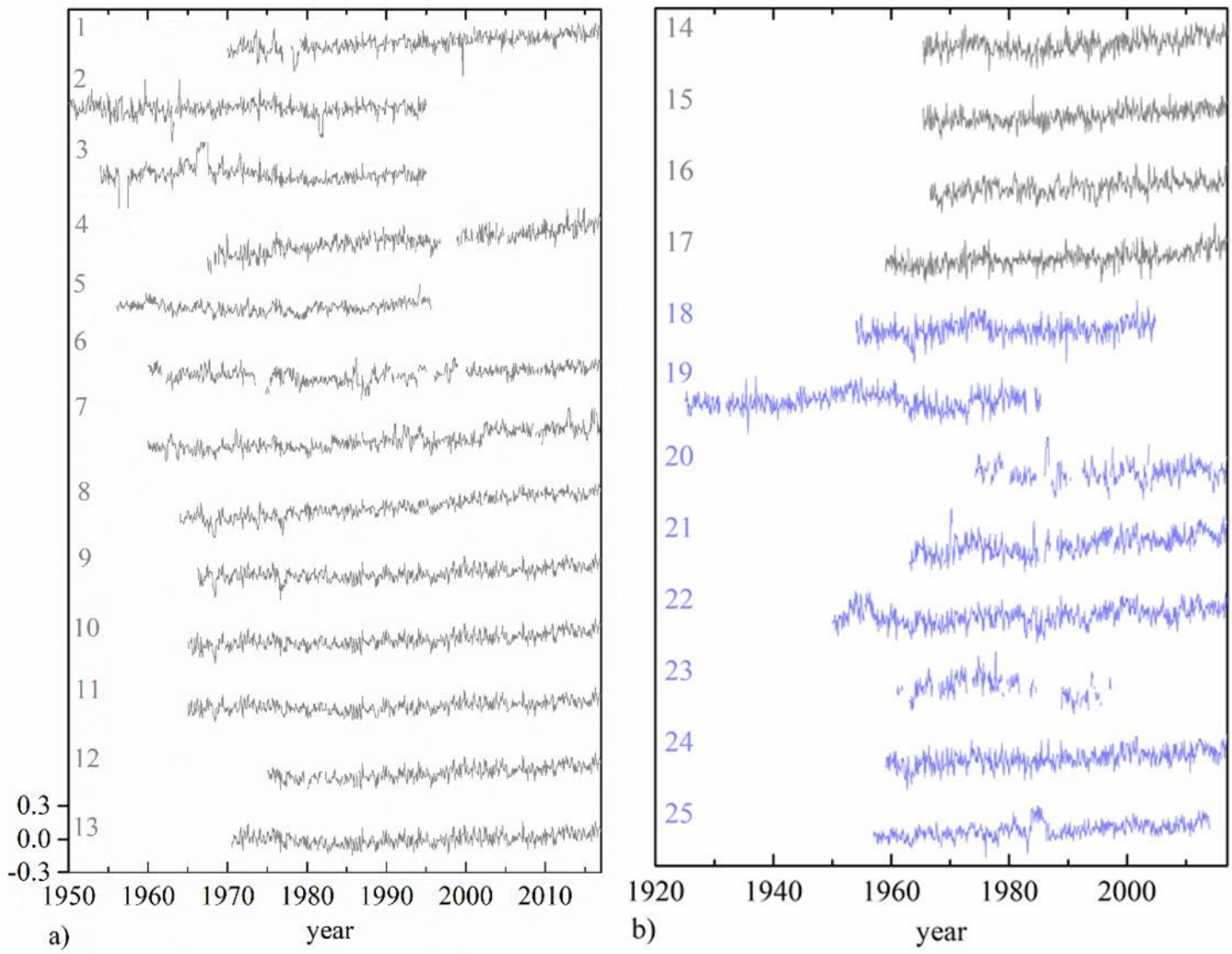

Figure 3

The monthly sea level change (SLC, Units: m) from all the tide gauge records in study area. Seasonal cycles are removed from all series.

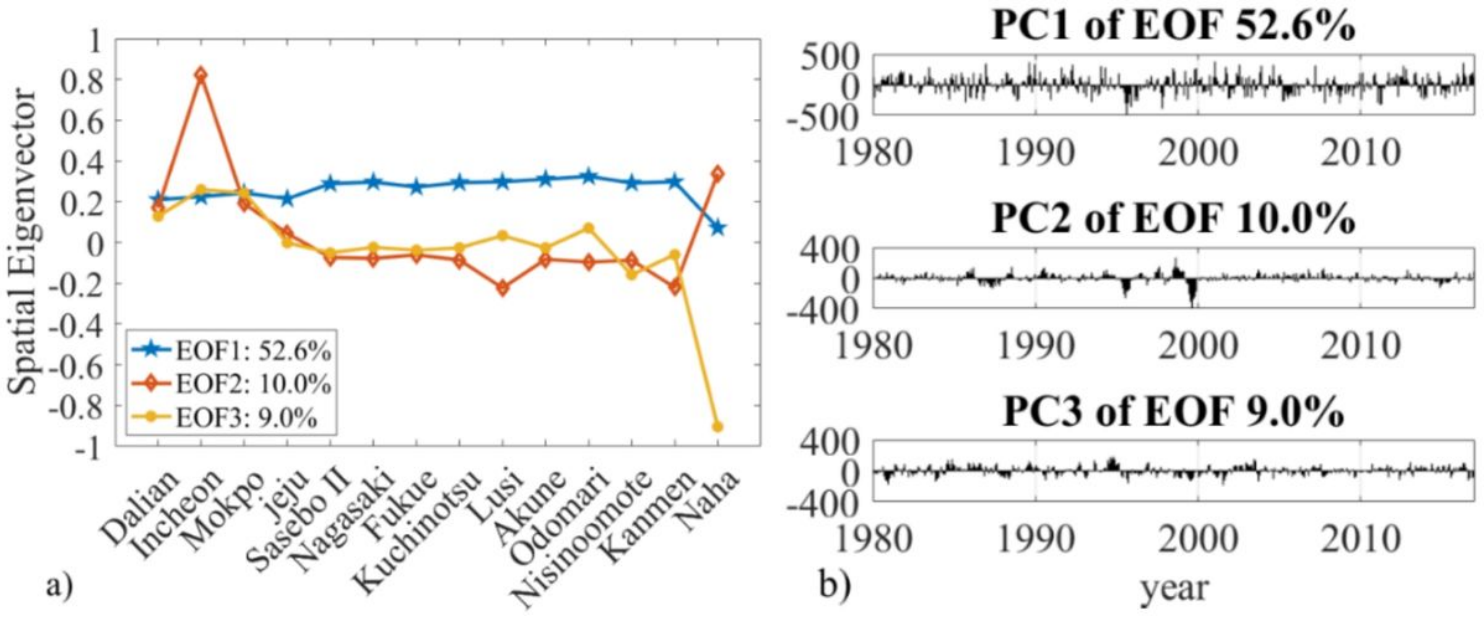

Figure 4

a) Spatial eigenvectors of the first three EOF modes of Region 1 b) Amplitudes of the time series for the first three EOF modes of Region 1

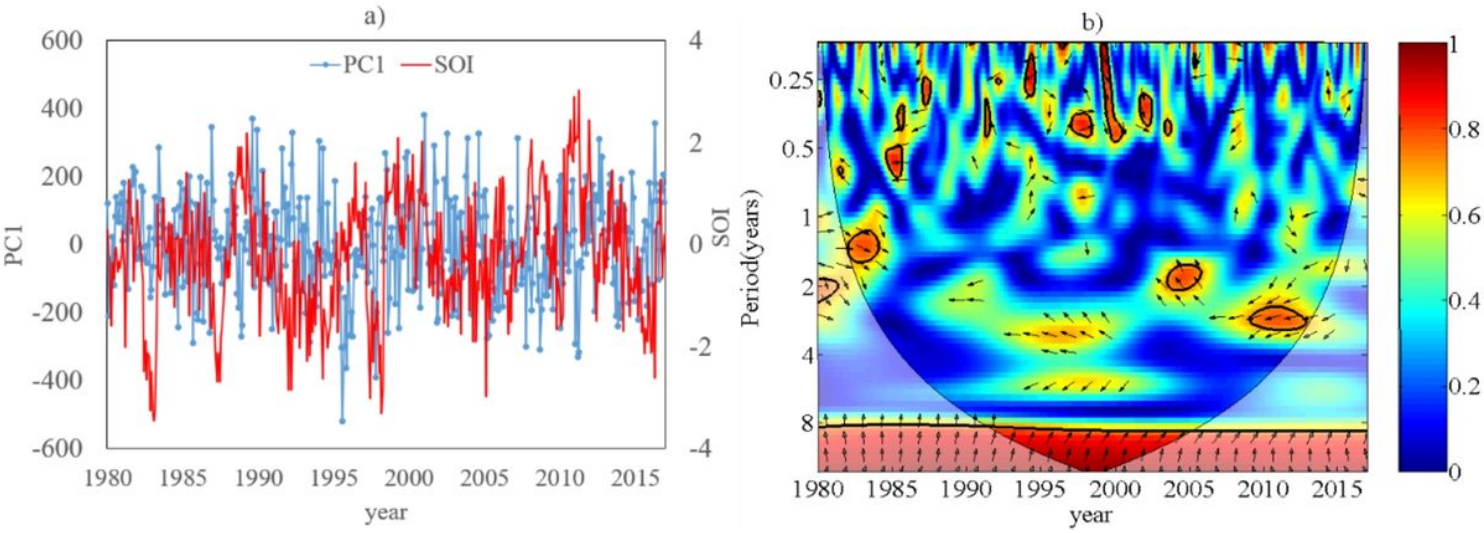

Figure 5

a) Comparison of the PC1 time series of Region 1 with SOI b) Wavelet coherence between PC1 time series of Region 1 and SOI (The vectors indicate the phase difference between two series, the horizontal arrow pointing left denotes in-phase, pointing right denotes anti-phase, pointing straight up denotes the first series leads the second by 90°)

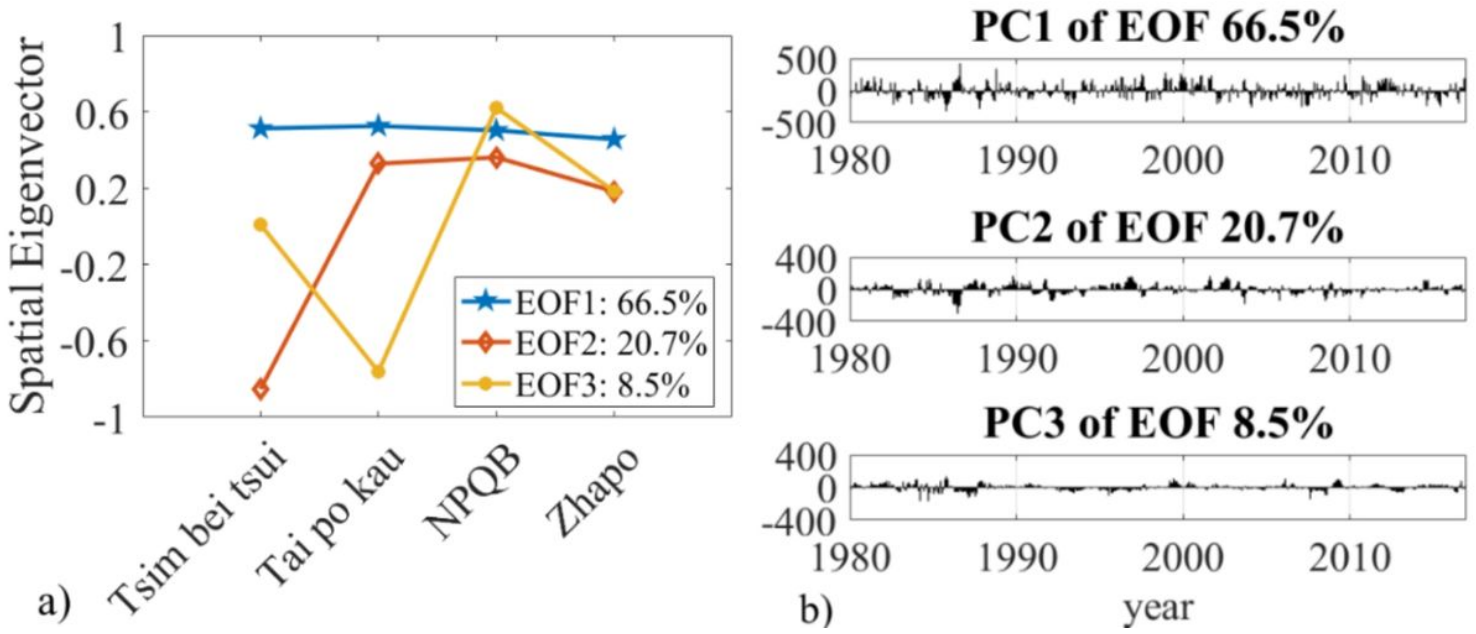

Figure 6

a) Spatial eigenvectors of the first three EOF modes of Region 2 b) Amplitudes of the time series for the first three EOF modes of Region 2

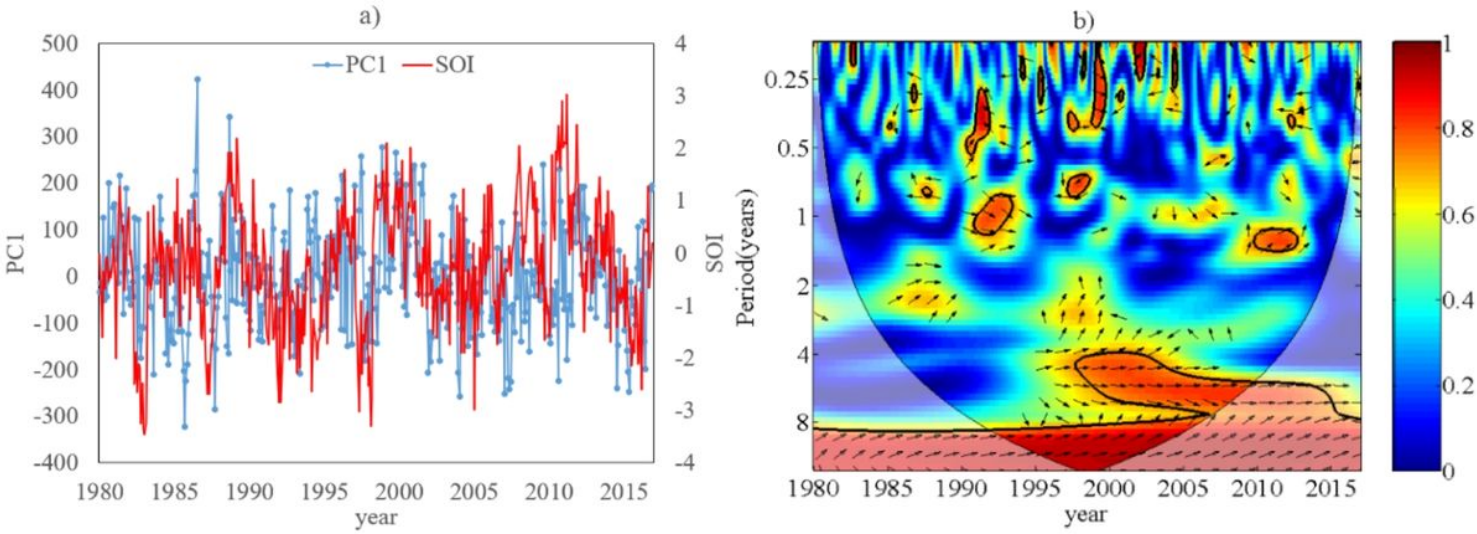

Figure 7

a) Comparison of the PC1 time series of Region 2 with SOI b) Wavelet coherence between PC1 time series of Region 2 and SOI

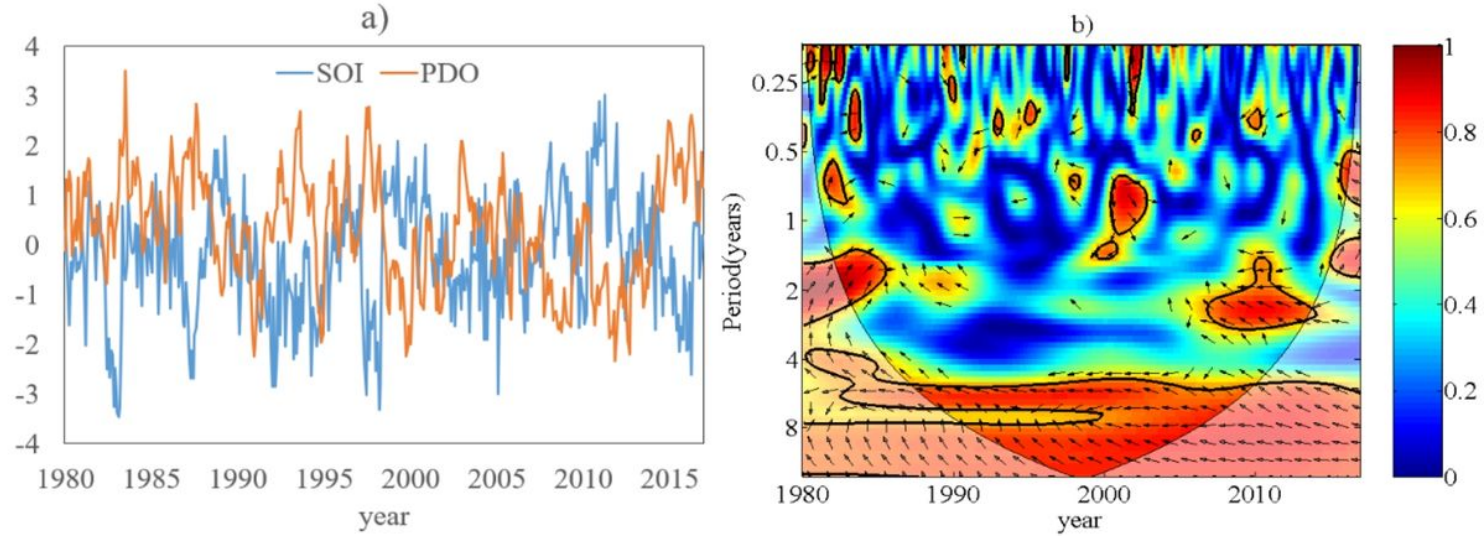

Figure 8

a) Comparison of SOI with PDO time series of Region 2 b) Wavelet coherence between SOI and PDO time series

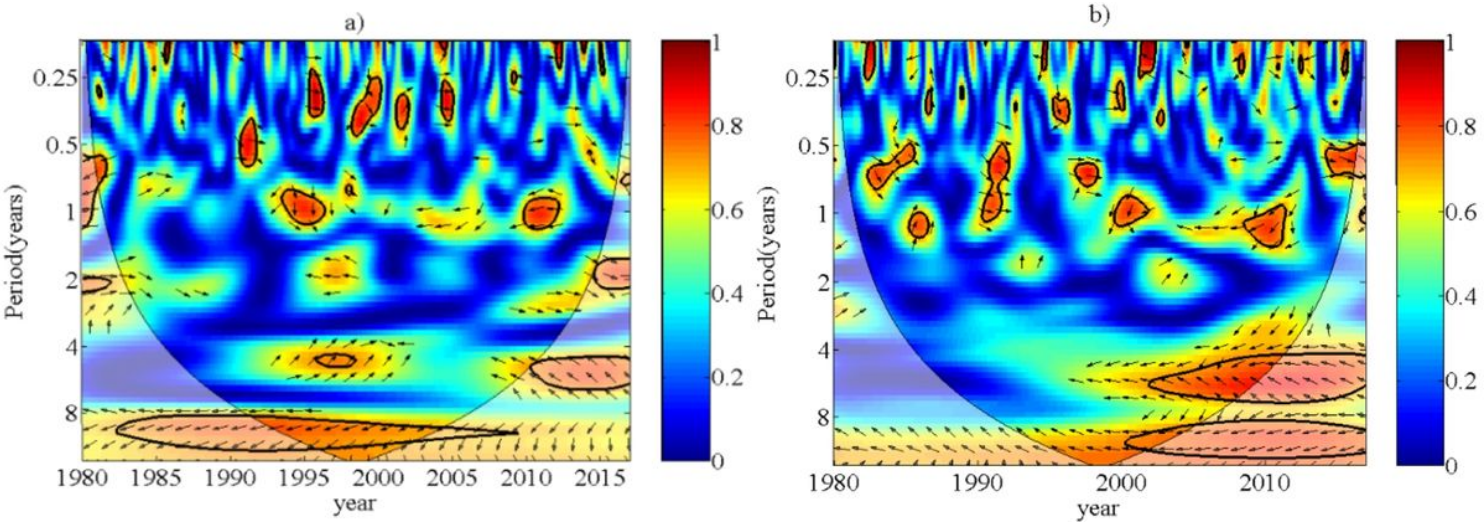

Figure 9

a) Wavelet coherence between PC1 time series of Region 1 with PDO b) Wavelet coherence between PC1 time series of Region 2 with PDO